Analysis of Iterative Multi-User Detection Schemes with EXIT Charts

Volker Kühn
Universität Bremen (Germany)
Department of Communications Engineering
Otto-Hahn-Allee NW 1, D-28359 Bremen
kuehn@ant.uni-bremen.de

***Abstract*— In the last years, CDMA has been established as a standard multiple access scheme in mobile radio communications. However, high spectral efficiency can only be achieved by applying multi-user detection schemes combatting the inherent multi-user interference. Since the optimum maximum likelihood approach is far to complex for practical implementations, suboptimum iterative strategies are applied. These iterative strategies follow the turbo principle well-known from coding theory and can be analyzed by means of extrinsic information transfer (EXIT) charts.**

This paper analyzes the performance of iterative multi-user detection schemes by EXIT charts. For simplicity, an AWGN channel and a synchronous transmission are assumed. Starting with optimum APP components, we show that the performance of the iterative scheme is well predictable by the EXIT chart technique. Results for different signal to noise ratios are presented. For non-ideal components like the parallel interference cancellation, the prediction becomes less accurate but is still possible.

I. Introduction

Code Division Multiple Access (CDMA) has become a widely accepted multiple access technique in mobile radio communications. Considering the uplink transmission, the orthogonality of spreading codes cannot be maintained and random spreading sequences are often used. Hence, multi-user interference is the limiting factor of the system performance. However, spectral efficiency can be increased by applying multi-user detection (MUD) techniques. In the last years, plenty of work has been spent on this topic, especially on iterative MUD techniques [1], [2], [3], [4], [5], [6], [7], [8], [9], [10], [11], [12]. However, there are still a lot of open questions concerning the convergence behavior of these iterative schemes.

In 1993, turbo codes were presented for the first time [13] and attracted great attention due to their amazing performance. In subsequent years, one tried to understand the way how turbo decoding works and why it performs so well. A key approach was presented by Stephan ten Brink [14], [15], [16], [17], [18] in 2000. He introduced the so called EXtrinsic Information Transfer (EXIT) charts with which a prediction of the convergence behavior of turbo decodes can be accurately predicted. However, the application of EXIT charts is not restricted to the decoding of concatenated codes but also suited for the concatenation of different components.

This paper considers the uplink of a coded direct-sequence CDMA system. Since the focus of this work is the performance analysis of iterative schemes based on information theory, we keep the system as simple as possible. Therefore, we assume a synchronous system without fading or near-far effects that is simply disturbed by an AWGN channel. The receiver consists of a serial concatenation of a block performing some appropriate processing to combat multi-user interference and a parallel arrangement of individual channel decoders.

The paper is structured as follows: Section 2 describes the considered DS-CDMA system. Next, section 3 presents two different iterative approaches for combatting the multi-user interference. Sections 4 and 5 introduce the EXIT chart analysis and evaluate the two approaches by comparing semi-analytical and simulation results. Section 6 gives a conclusion.

II. System Description

The structure of the considered DS-CDMA system is depicted in Fig. 1. The information bits $d_u[i]$ of each user u, $1 \leq u \leq U$, are first encoded by identical convolutional codes of rate $R_c = 1/n$ and constraint length L_c. The resulting code bits are BPSK modulated and interleaved by user-specific interleavers Π_u of length L_π. Next, direct-sequence spreading by a factor N_s is carried out with pseudo random codes $\mathbf{c}_u[k] = \big[c_{u,1}[k] \cdots c_{u,N_s}[k]\big]^T$ whose binary chips can take the values $c_{u,\ell}[k] = \pm 1$. The system load is one of the key parameters and defined to $\beta = U/N_s$.

At the receiver, we obtain a superposition of all transmitted signals $\mathbf{x}_u[k] = \big[x_{u,1}[k] \cdots x_{u,N_s}[k]\big]^T$ and additive white gaussian noise $\mathbf{n}[k]$ with power σ_n^2. Comprising all spreading codes $\mathbf{c}_u[k]$ in a matrix $\mathbf{C}[k] = \big[\mathbf{c}_1[k] \cdots \mathbf{c}_U[k]\big]$ and the coded BPSK symbols of all users in a vector $\mathbf{b}[k] = \big[b_1[k] \cdots b_U[k]\big]^T$, the k-th received vector can be expressed by

$$\mathbf{y}[k] = \mathbf{C}[k] \cdot \mathbf{b}[k] + \mathbf{n}[k] \,. \tag{1}$$

Despreading is performed by passing $\mathbf{y}[k]$ through a bank of matched filters, one for each user. We obtain

$$\mathbf{r}[k] = \mathbf{C}^T[k] \cdot \mathbf{y}[k] = \mathbf{R}[k] \cdot \mathbf{b}[k] + \tilde{\mathbf{n}}[k] \tag{2}$$

where $\mathbf{R}[k] = \mathbf{C}^T[k] \cdot \mathbf{C}[k]$ is the correlation matrix and $\tilde{\mathbf{n}}[k] = \mathbf{S}^T[k] \cdot \mathbf{n}[k]$ denotes the modified noise vector with

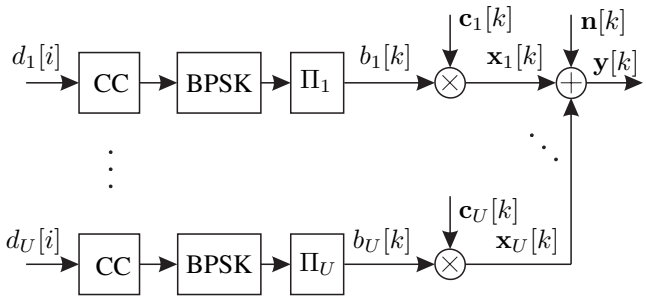

Fig. 1. Transmitter structure of coded DS-CDMA system

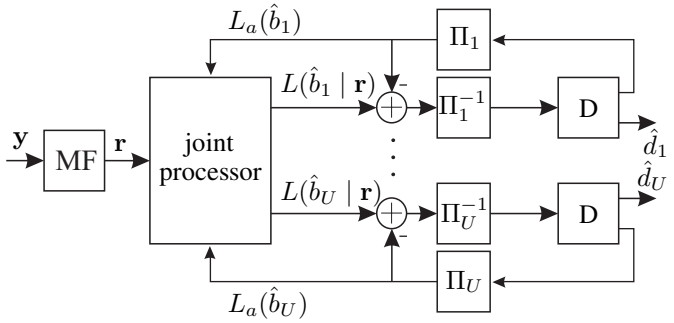

Fig. 2. Iterative receiver structure of coded DS-CDMA system (time instances neglected)

instantaneous covariance matrix $\mathbf{\Phi}_{\tilde{n}\tilde{n}}[k] = E\{\tilde{\mathbf{n}}[k]\tilde{\mathbf{n}}^T[k]\} = \sigma_n^2 \cdot \mathbf{R}[k]$.

The vector $\mathbf{r}[k]$ at the output of the matched filter bank represents a sufficient statistics, i.e. the whole information contained in $\mathbf{y}[k]$ is maintained and an optimum decision is still possible. However, optimum maximum likelihood detection of the information bits $d_u[i]$ for all users is infeasible in practice. Therefore, we consider an iterative approach that separates the CDMA specific part from the conventional channel decoder as depicted in Fig. 2. The matched filter output is processed by a device called joint processor delivering a soft estimate for each user symbol $b_u[k]$. Details about the algorithm are given in the next section.

After de-interleaving, each sequence is decoded by a soft-in/soft-out decoder, e.g. a BCJR algorithm [19]. It delivers estimates $\hat{d}_u[i]$ of the information bits $d_u[i]$ as well as log-likelihood values $L(\hat{b}_u[k])$ of the coded bits $b_u[k]$. The latter one is interleaved and fed back as a priori information $L_a(\hat{b}_u[k])$ to the joint processor. Now, the procedure is repeated according to the turbo principle [13] until a stopping criterion is fulfilled.

III. Joint Processing

A. Optimum Joint Processor

Due to binary BPSK symbols, the optimum soft information at the output of the joint processor can be described by a log likelihood ratio

$$L(\hat{b}_u[k] \mid \mathbf{r}[k]) = \log \frac{\Pr\{b_u[k] = +1 \mid \mathbf{r}[k]\}}{\Pr\{b_u[k] = -1 \mid \mathbf{r}[k]\}} \,. \tag{3}$$

Extending the probabilities in nominator and denominator of (3) and applying Bayes rule results in

$$\begin{aligned} L(\hat{b}_u[k] \mid \mathbf{r}[k]) &= \log \frac{\sum_{\tilde{\mathbf{b}},\tilde{b}_u=+1} \Pr\{\tilde{\mathbf{b}} \mid \mathbf{r}[k]\}}{\sum_{\tilde{\mathbf{b}},\tilde{b}_u=-1} \Pr\{\tilde{\mathbf{b}} \mid \mathbf{r}[k]\}} \\ &= \log \frac{\sum_{\tilde{\mathbf{b}},\tilde{b}_u=+1} p(\mathbf{r}[k] \mid \tilde{\mathbf{b}}) \cdot \Pr\{\tilde{\mathbf{b}}\}}{\sum_{\tilde{\mathbf{b}},\tilde{b}_u=-1} p(\mathbf{r}[k] \mid \tilde{\mathbf{b}}) \cdot \Pr\{\tilde{\mathbf{b}}\}} \end{aligned} \tag{4}$$

In (4), the sums run over all possible transmit vectors $\tilde{\mathbf{b}} = [\tilde{b}_1 \cdots \tilde{b}_U]$ so that the computational effort growths exponentially with the number of users U. Nevertheless, it represents the optimum soft output information [4], [5]. In a first stage, no a priori information $\Pr\{\tilde{\mathbf{b}}\}$ is available. The multivariate conditional distribution of $\mathbf{r}[k]$ can be expressed by[1]

$$\begin{aligned} p(\mathbf{r} \mid \tilde{\mathbf{b}}) &= \frac{1}{\det(\pi \mathbf{\Phi}_{\tilde{n}\tilde{n}})} \cdot e^{-(\mathbf{r}-\mathbf{R}\tilde{\mathbf{b}})^T \mathbf{\Phi}_{\tilde{n}\tilde{n}}^{-1}(\mathbf{r}-\mathbf{R}\tilde{\mathbf{b}})} \\ &= K \cdot e^{-(2\mathbf{r}^T - \tilde{\mathbf{b}}^T\mathbf{R})\tilde{\mathbf{b}}/\sigma_n^2} \end{aligned} \tag{5}$$

where K comprises all terms independent from $\tilde{\mathbf{b}}$. Inserting (5) into (4) and neglecting the a priori probabilities $\Pr\{\tilde{\mathbf{b}}\}$ yields

$$L(\hat{b}_u \mid \mathbf{r}) = \log \frac{\sum_{\tilde{\mathbf{b}},\tilde{b}_u=+1} e^{(2\mathbf{r}^T - \tilde{\mathbf{b}}^T\mathbf{R})\tilde{\mathbf{b}}/\sigma_n^2}}{\sum_{\tilde{\mathbf{b}},\tilde{b}_u=-1} e^{(2\mathbf{r}^T - \tilde{\mathbf{b}}^T\mathbf{R})\tilde{\mathbf{b}}/\sigma_n^2}} \,. \tag{6}$$

The LLR's in (6) represent the input of the u-th channel decoder in the first stage. After extracting the extrinsic part of the decoder's output, the joint processor can exploit it as priori information $L_a(\hat{b}_u)$ in subsequent iterations. Since the symbols b_u of different users u are statistically independent, the relation between extrinsic LLR's and a priori probabilities is given by [20]

$$\Pr\{\mathbf{b}\} = \prod_{u=1}^{U} \Pr\{b_u\} = \prod_{u=1}^{U} \frac{e^{b_u L_a(\hat{b}_u)/2}}{1 + e^{L_a(\hat{b}_u)/2}} \,. \tag{7}$$

The denominator in (7) does not depend on the value of $\tilde{b}_u$ and cancels when inserting (7) into (6). Hence, the output of the joint processor for the second and all subsequent iterations becomes

$$\begin{aligned} &L\,(\hat{b}_u \mid \mathbf{r}) \\ &= \log \frac{\sum_{\tilde{\mathbf{b}},\tilde{b}_u=+1} e^{(2\mathbf{r}^T - \tilde{\mathbf{b}}^T\mathbf{R})\tilde{\mathbf{b}}/\sigma_n^2} \prod_{v=1}^{U} e^{\tilde{b}_v L_a(\hat{b}_v)/2}}{\sum_{\tilde{\mathbf{b}},\tilde{b}_u=-1} e^{(2\mathbf{r}^T - \tilde{\mathbf{b}}^T\mathbf{R})\tilde{\mathbf{b}}/\sigma_n^2} \prod_{v=1}^{U} e^{\tilde{b}_v L_a(\hat{b}_v)/2}} \\ &= L_a(\hat{b}_u) + \\ &\quad \log \frac{\sum_{\tilde{\mathbf{b}},\tilde{b}_u=+1} e^{(2\mathbf{r}^T - \tilde{\mathbf{b}}^T\mathbf{R})\tilde{\mathbf{b}}/\sigma_n^2 + \sum_{\substack{v=1 \\ v\neq u}}^{U} \tilde{b}_v L_a(\hat{b}_v)/2}}{\sum_{\tilde{\mathbf{b}},\tilde{b}_u=-1} e^{(2\mathbf{r}^T - \tilde{\mathbf{b}}^T\mathbf{R})\tilde{\mathbf{b}}/\sigma_n^2 + \sum_{\substack{v=1 \\ v\neq u}}^{U} \tilde{b}_v L_a(\hat{b}_v)/2}} \,. \end{aligned} \tag{8}$$

Obviously, $L(\hat{b}_u \mid \mathbf{r})$ can be split into an a priori part $L_a(\hat{b}_u)$ and an extrinsic part. The first one has to be subtracted before the signal is fed back to the channel decoder that generated it (compare Fig. 2).

[1] For notational simplicity, we drop the time instance k in the sequel.

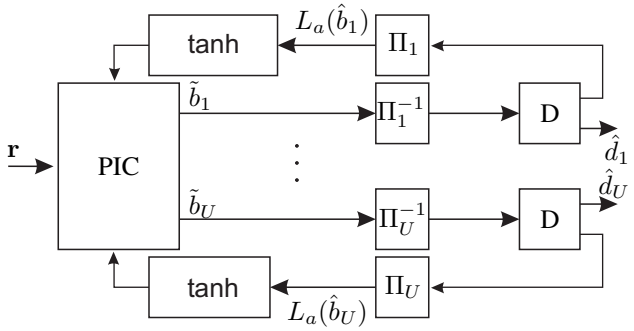

Fig. 3. Receiver structure for PIC (time instances neglected)

B. Parallel Interference Cancellation

Since the computational effort becomes quickly infeasible when the number of users increases, the optimum joint processor is restricted to very small systems with only a few users. However, there exist suboptimum approaches whose complexity growths only linearly with the number of users. One example is the parallel interference cancellation [21]. It was chosen because all users are processed parallely in the same way so that the mutual information in each user stream is the same. This greatly simplifies the analysis in the next sections.

The whole receiver structure is depicted in Fig. 3. In the first stage, the PIC block is passive because no a priori knowledge is available and the matched filter outputs are directly fed to the channel decoders. Their outputs are deinterleaved and fed back as a priori LLR's $L_a(\hat{b}_u[k])$. Before they enter the joint processor, the $\tanh$-function is applied delivering expected values [20]. The block PIC now performs a simple interference cancellation according to

$$\tilde{b}_u[k] = 4\frac{E_s}{N_0} \cdot \left[r_u[k] - \sum_{\substack{v=1 \\ v \neq u}}^{U} \tanh\left(L_a(\hat{b}_u[k])/2 \right) \right] . \quad (9)$$

Obviously, $\tilde{b}_u[k]$ does only depend on $r_u[k]$ and not on the whole vector $\mathbf{r}[k]$. Assuming that interference has been totally cancelled, only the noise disturbs the transmission and a log-likelihood ratio $L(\hat{b}_u[k] \mid r_u[k])$ is obtained by weighting $\tilde{b}_u[k]$ with the scalar $4E_s/N_0$. Certainly, this is only an approximation and not exactly a log-likelihood ratio.

IV. EXIT Chart Analysis

EXtrinsic Information Transfer (EXIT) charts are an appropriate mean to analyze the convergence behavior of iterative schemes. In [14]-[18], various examples for serial and parallel concatenated codes are presented. In the context of this paper, we consider a serial concatenation of a joint processor and a set of independently operating channel decoders (see Figs. 2 and 3). The basic idea behind EXIT charts is the exchange of mutual information between the components of a concatenated system. Generally, the mutual information between a binary

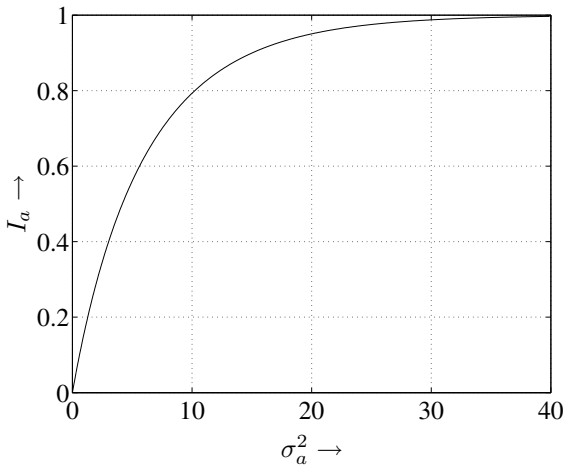

Fig. 4. Mutual information versus a priori variance σ_a^2

signal x and a continuously distributed signal y is defined to

$$I(x;y) = 1 + \frac{1}{2} \cdot \sum_{d=\pm 1} \int_{-\infty}^{\infty} p(y \mid x = d) \times \log \frac{p(y \mid x = d)}{p(y \mid x = 1) + p(y \mid x = -1)} dy . \quad (10)$$

Following the approach of Stephan ten Brink, we assume that the a priori LLR's $L_a(\hat{b}_u)$ can be modelled as a superposition of the transmitted data symbols b_u and white gaussian noise

$$L_a(\hat{b}_u) = \overline{n}_u b_u + n_u . \quad (11)$$

In (11), n_u denotes the white gaussian noise with variance σ_a^2. The mean of $L_a(\hat{b}_u)$ is $\overline{n}_u = \sigma_a^2/2$ [18]. The mutual information between $L_a(\hat{b}_u)$ and the true $b_u = \pm 1$ is obtained by applying (10)

$$I(L_a(\hat{b}_u); b_u) = 1 - \frac{1}{\sqrt{2\pi\sigma_a^2}} \cdot \int_{-\infty}^{\infty} e^{-\frac{(\xi - \sigma_a^2/2)^2}{2\sigma_a^2}} \log(1 + e^{-\xi}) d\xi \quad (12)$$

and depends only on the variance σ_a^2. The relation is depicted in Fig. 4.

The mutual information at the input of each component is always modelled in the form of (11). Contrarily, the mutual information between b_u and the output of a device cannot be expressed in that way. In fact, the probability density $p(y \mid x)$ has to be estimated by calculating a histogram $\hat{p}(y \mid x)$. In total, we obtain 4 different mutual informations:

$$I_{a,u}^{jp} = I\big(L_a(\hat{b}_u); b_u\big) \quad (13a)$$

$$I_{e,u}^{jp} = I\big(L(\hat{b}_u \mid \mathbf{r}) - L_a(\hat{b}_u); b_u\big) \quad (13b)$$

$$I_{a,u}^{D} = I_{e,u}^{jp} \quad (13c)$$

$$I_{t,u}^{D} = I_{a,u}^{jp} . \quad (13d)$$

$I_{a,u}^{jp}$ in (13a) describes the mutual information of the u-th joint processor input and (13b) the extrinsic part of the corresponding output. The latter one is exactly the a priori information at the u-th decoder input (see (13c)) because interleaving does not affect the information. With the same

argumentation, the information at the u-th decoder output becomes the u-th contribution to the a priori information of the joint processor (see (13d))[2]. The total mutual a priori information of this device is

$$I_a^{jp} = \sum_{u=1}^{U} I(L_a(\hat{b}_u); b_u) \tag{14}$$

because the user-specific interleaving ensures independence between the signals in different user branches and the corresponding mutual informations can be simply summed.

V. Results

In order to evaluate the application of EXIT charts to iterative multi-user detection schemes, we consider the following system model. The information bits are first encoded by a half rate convolutional code with constraint length $L_c = 3$ and generators $g_1 = 5_8$ and $g_2 = 7_8$. The length of the interleaver is $L_\pi = 30000$. Pseudo random long codes are used for spreading with a factor $N_s = 4$ and $U = 4$ users lead to a load of $\beta = 1$.

Since all users are affected in the same way by interference and noise and are processed in a parallel manner, we have a perfect symmetry and the mutual a priori and extrinsic informations are identical for all users. Therefore, we use the average mutual informations

$$\overline{I}_a^{jp} = \frac{1}{U} \cdot I_a^{jp} = \frac{1}{U} \cdot \sum_{u=1}^{U} I(L_a(\hat{b}_u); b_u) \tag{15}$$

and

$$\overline{I}_e^{jp} = \frac{1}{U} \cdot \sum_{u=1}^{U} I_{e,u}^{jp} \tag{16}$$

at input and output of the joint processor, respectively. For all simulations, a maximum number of 10 iterations was carried out.

A. Optimal Joint Processor

Fig. 5 shows the transfer characteristic of the optimum joint processor derived in Section III-A for a system load of $\beta = 1$. Obviously, the mutual information strongly depends on the signal to noise ratio. The higher E_s/N_0, the larger is the mutual information at the processor's output. For perfect a priori information $\overline{I}_a^{jp} = 1$, the interference is totally suppressed and we obtain a single-user AWGN system. Hence, the extrinsic mutual information at the output equals the channel capacity $C(E_s/N_0)$. In this case, additional iterations do not lead to further improvements.

The convolutional code used in our simulations is also shown in Fig. 5. At low signal to noise ratios, we observe an early intersection with the trajectories of the joint processor and iterations get stuck. Fig. 6 shows the EXIT chart at a signal to noise ratio of 0 dB. Except the starting point that exceeds the

[2]As opposed to classical turbo decoding where only extrinsic information is exchanged, we use the entire decoder outputs to provide a priori knowledge I_t^D to the multi-user detector.

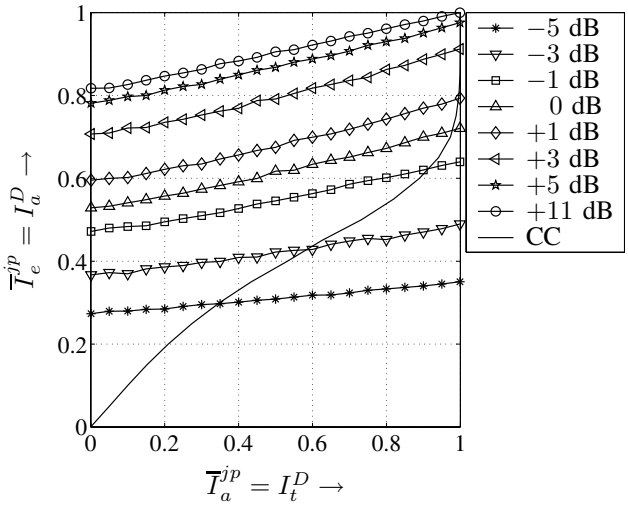

Fig. 5. Transfer characteristic for optimum joint processor and different E_s/N_0 values, load $\beta = 1$

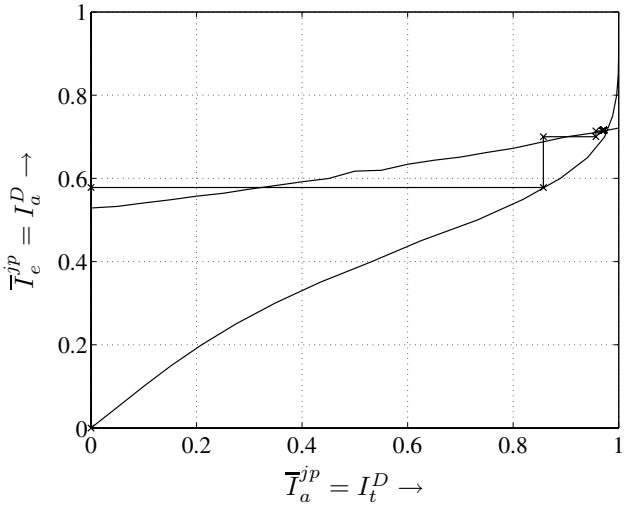

Fig. 6. EXIT chart for optimum joint processor at $E_s/N_0 \hat{=} 0$ dB

trajectories a good match between predicted and true behavior of the iterative process can be observed. The iterative scheme converges up to the intersection of the trajectories.

B. Parallel Interference Cancellation

Fig. 7 shows the corresponding transfer charts for parallel interference cancellation. Comparing the results with Fig. 5 we observe that the slope of the curves is much steeper. The final extrinsic information for $\overline{I}_a^{jp} = 1$ is the same as for the optimum joint processor but the starting point for low a priori information is much worse. While the results are quite similar for very low SNR, the differences between the curves increase at higher signal to noise ratios and low $\overline{I}_a^{jp}$. This implies that – depending on the choice of the error correcting code – higher SNRs and more iterations are needed to get convergence.

The corresponding EXIT chart is shown in Fig. 8 for $E_s/N_0 \hat{=} 10$ dB. We observe deviations from the predicted convergence behavior and the iterative process gets stuck

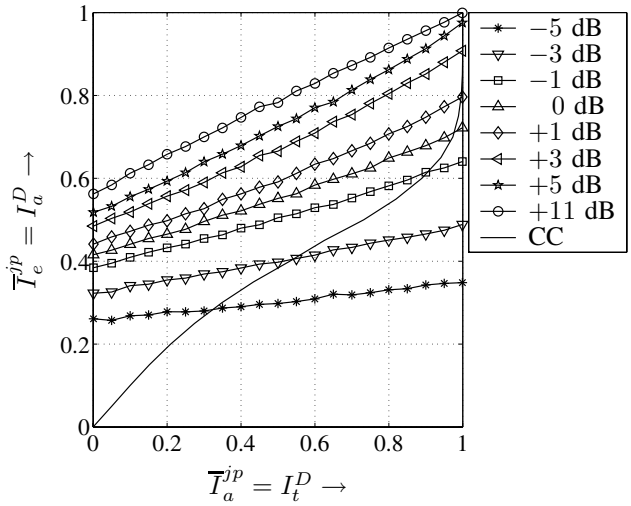

Fig. 7. Transfer characteristic for PIC and different E_s/N_0 values

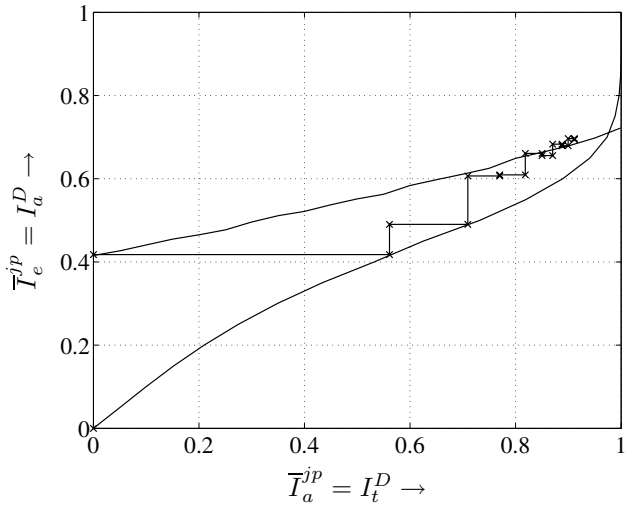

Fig. 8. EXIT chart for parallel interference cancellation at $E_s/N_0 \hat{=} 0$ dB

before reaching the intersection. However, a certain prediction is still possible because the deviations are relatively small.

VI. Conclusion

It was shown that EXIT charts are an appropriate mean to analyze the convergence behavior of iterative multi-user detection schemes. The mutual information at the output of the MUD device depends on the signal to noise ratio and reaches the channel capacity for perfect a priori information. Applying the optimum joint processor, a tight prediction of the convergence behavior is possible. For low cost approximations like the parallel interference cancellations, slight deviations are observed. However, a less accurate prediction is still possible.

Further work has to be performed on the optimization of channel codes with respect to a good convergence of the iterative scheme. Moreover, successive interference cancellation prohibiting simple averaging of mutual informations should be considered. This is especially important for near-far scenarios or multi-rate systems where the mutual information varies from user to user.

References

[1] S. Moshavi. Multi-User Detection for DS-CDMA Communications. *IEEE Communications Magazine*, pages 124–136, Oktober 1996.

[2] L.B. Nelson and V. Poor. Iterative Multiuser Receivers for CDMA Channels: An EM-based Approach. *IEEE Transactions on Communications*, 44(12):1700–1710, December 1996.

[3] S. Verdu. *Multiuser Detection*. Cambridge University Press, New York, 1998.

[4] M.C. Reed, C.B. Schlegel, P.D. Alexander, and J.A. Asenstorfer. Iterative Multiuser Detection for CDMA with FEC: Near-Single-User Performance. *IEEE Transactions on Communications*, 46(12):1693–1699, December 1998.

[5] P.D. Alexander, M.C. Reed, J.A. Asenstorfer, and C.B. Schlegel. Iterative Multiuser Interference Reduction: Turbo CDMA. *IEEE Transactions on Communications*, 47(7):1008–1014, Juli 1999.

[6] S. Verdu and S. Shamai. Spectral Efficiency of CDMA with Random Spreading. *IEEE Transactions on Information Theory*, 45(2):622–640, März 1999.

[7] P. Schramm and R.R. Müller. Spectral Efficiency of CDMA Systems with Linear MMSE Interference Suppression. *IEEE Transactions on Communications*, 47(5):722–731, May 1999.

[8] D. Tse and S.V. Hanly. Linear Multiuser Receivers: Effective Interference, Effective Bandwidth and User Capacity. *IEEE Transactions on Information Theory*, 45(2):641–657, März 1999.

[9] M. Honig and M.K. Tsatsanis. Multiuser CDMA Receivers. *IEEE Signal Processing Magazine*, pages 49–61, May 2000.

[10] M. Kobayashi, J. Boutros, and G. Caire. Successive Interference Cancellation with SISO Decoding and EM Channel Estimation. *IEEE Journal on Selected Areas in Communications*, 19(8):1450–1460, August 2001.

[11] A. Lampe, R. Schober, W. Gerstacker, and J. Huber. A Novel Multiuser Detector for Complex Modulation Schemes. *IEEE Journal on Selected Areas in Communications*, 20(2):339–349, February 2002.

[12] A. Lampe and J. Huber. Iterative Interference Cancellation for DS-CDMA Systems with High System Loads Using Reliability-Dependent Feedback. *IEEE Transactions on Vehicular Technology*, 51(3):445–452, May 2002.

[13] C. Berrou, A. Glavieux and P. Thitimajshima. Near Shannon Limit Error-Correcting Coding and Decoding: Turbo-Codes (1). *IEEE Proc. International Conference on Communications*, pages 1064–1070, Geneva, 1993.

[14] S. ten Brink. Iterative Decoding Trajectories of Parallel Concatenated Codes. *IEEE/ITG Conference on Source and Channel Coding*. pages 75–80, Munich, January 2000.

[15] S. ten Brink. Rate one-half code for approaching the Shannon limit by 0.1 dB. *Electronics letters*. 36(15):1293–1294, July 2000.

[16] S. ten Brink. Code Characteristic Matching for Iterative Decoding of Serially Concatenated Codes. *Annales des Telecommunication*. pages 100–110, 2001.

[17] S. ten Brink. Code doping for triggering iterative decoding convergence. *IEEE Proc. International Symposium on Information Theory*. pages 235–235, 2001.

[18] S. ten Brink. Convergence Behavior of Iteratively Decoded Parallel Concatenated Codes. *IEEE Transactions on Communications*. 49(10):1727–1737, October 2001.

[19] L.R. Bahl, J. Cocke, F. Jelinek and J. Raviv. Optimal Decoding of Linear Codes for Minimizing Symbol Error Rate. *IEEE Transactions on Information Theory*. 20:248–287, March 1974.

[20] J. Hagenauer. SSource-controlled channel decoding. *IEEE Transactions on Communications*. 43(9):2449–2457, September 1996.

[21] V. Kühn. Combined MMSE-PIC in Coded OFDM-CDMA Systems. *IEEE Global Conference on Telecommunications*. San Antonio, USA, November 2001.